JACS Hosting Innovations

Contents List available at JACS Directory

# Journal of Advanced Electrochemistry

journal homepage: http://www.jacsdirectory.com/jaec



Influence of Doping Effect on The Infrared Spectra, X-Ray Powder Diffractogram and Thermal Spectra of  $[0.7(Ag_2HgI_4):0.3(AgI_x:CuI_{(1-x)})]$  of Fast-Ion Conductors (x = 0.2, 0.4, 0.6 and 0.8 mol. wt. %)

N. Saba\*, A. Ahmad

Solid State Chemistry Lab, Department of Chemistry, Aligarh Muslim University, Aligarh - 202 002, UP, India.

#### ARTICLE DETAILS

Article history:
Received 14 December 2015
Accepted 28 December 2015
Available online 07 February 2016

Keywords: Thermal Analysis Doping FTIR XRD

#### ABSTRACT

The origin and nature of correlation between silver and copper ion conduction and composition of various phases present in the mixed system  $[0.7(Ag_2HgI_4):0.3(AgI_x:CuI_{(1-x)})]$  (where x=0.2, 0.4, 0.6 and 0.8 mol. wt. %) were prepared by solid state reaction of the appropriate solid mixtures and quenching them at particular temperature. Powdered samples of different compositions containing x mol. wt. % of  $(AgI_x:CuI_{(1-x)})$  were synthesized by solid state reactions, using  $[Ag_2HgI_4]$  ternary halides as host. Powder specimens of these compositions were analyzed using Fourier transmission infrared spectra (FTIR), x-ray powder diffraction (XRD) differential thermal analysis (DTA), differential scanning calorimetry (DSC) and thermal gravimetric analysis (TGA) techniques. These studies have confirmed the formation of new products as revealed by the absence of diffraction peaks of parent materials in the XRD patterns. Among the various compositions, a significant number of peaks found to contain  $Ag^+$  and  $Cu^+$  in  $Ag_2HgI_4$  respectively and DSC traces have indicated the characteristic melting temperature of  $[0.7(Ag_2HgI_4):0.3(AgI_x:CuI_{(1-x)})]$  at around 527.8 K, 516.6 K, 586.8 K and 494.8 K in x=0.2, 0.4, 0.6 and 0.8 respectively. Fourier transmission infrared spectra of all the the fast ionic conductors  $[0.7(Ag_2HgI_4):0.3(AgI_x:CuI_{(1-x)})]$  provided assignment for the more prominent infrared spectra to specific irreducible representation.

#### 1. Introduction

Many fast ionic compounds including those belonging to the A2BX4 group (A = Ag and Cu, B = Cd and Hg, X = I) are usually obtained by means of ceramic technology [1-4]. Chemical substitution has been used extensively in recent years to modify either the magnitude of ionic conductivity or the transition temperature separating super ionic and covalent phases in various solid electrolytes [5]. Present work is based on the study of some nominal compositions of  $[0.7(Ag_2HgI_4):0.3(AgI_x:CuI_{(1-x)})$ where x = 0.2, 0.4, 0.6 and 0.8 mol. wt. % respectively using the Fourier transmission infrared spectra (FTIR), x-ray powder diffraction (XRD differential thermal analysis (DTA), differential scanning calorimetry (DSC) and thermal gravimetric analysis (TGA),) techniques. Silver mercury tetraiodides have long been known to be both fast ion conductors [6, 7] and thermochromic pigments [8, 9]. Because Ag<sub>2</sub>HgI<sub>4</sub> have phase transitions in the 50-55°C range involving color changes and large changes in ionic conductivity, these thermochromic materials have also been proposed for various sensors. Recently, the mechanism for the presence or absence of thermochromism in analogues of Ag2HgI4 above and below their phase transition temperature has been reported [9]. The temperature dependent thermochromism is due to changes in the charge transfer spectra arising from the donation of electron charge from the filled p-orbitals of the iodide ligands to the unfilled d-orbitals of the mercury atom. The phase transition is considered to be an order-disorder type. The low temperature, β-phase of Ag<sub>2</sub>HgI<sub>4</sub> is tetragonal but they differ in the placement of the A+ cations and vacancy. In the high temperature,  $\alpha$ phase, the iodide sublattice is retained while cations are distributed randomly among all sites. Thus, they Ag<sub>2</sub>HgI<sub>4</sub> is isostructural in their αphases, clearly, them, the A+ cations plays a role in the exact structure in the low temperature form and determines, for the most part, the conductivity, phase transition temperature and thermo chromic properties [10]. We have undertaken a study of the synthesis and

properties of the analogues of  $A_2BX_4$  with the overall objective to finetune the structural, spectral and thermal properties of  $Ag_2HgI_4$  compounds with the choice of  $A^{\star}$  and possible mixed (Ag\*:Cu\*) substitutions to obtain materials useful for sensors and others electrochemical devices.

Although the initial purpose of this work is to see cations double (Ag\*:Cu\*) effect by introducing in  $A_2BX_4$  systems, we find that it is quite difficult to see this and instead we find the structure of pure  $A_2BX_4$  systems is different from iodide fast ionic system leading to the phase separation structure.

## 2. Experimental Methods

#### 2.1 Materials

The following materials were used as received; mercury [II] iodide, cuprous iodide and silver iodide were of CDH anal grade (India), each of which had a purity of 99%, 99% and 99% respectively.

2.2 Preparation of Pure and Doped Samples of [0.7(Ag2HgI4):0.3(AgIx:CuI $_{(1-x)}$ )]

## 2.2.1 Preparation of Pure Sample [Ag2HgI4]

Silver tetramercuroiodate [Ag<sub>2</sub>HgI<sub>4</sub>] was prepared by the conventional solid state reaction from AgI and HgI<sub>2</sub> (CDH, India), with stated purity of 99.5 respectively. Both reactants i.e. AgI and HgI<sub>2</sub> were mixed thoroughly in a requisite composition in an Agate mortar (each above 300 mesh size). The fine ground stoichiometric mixture of the binary component was sealed in an ampoule and was placed in air oven (CE 0434 NSW- 144) at about 100 °C (373 K) for 5 days. After cooling, a dark yellow color compound was formed which is changed to orange yellow. Ag<sub>2</sub>HgI<sub>4</sub> is orange yellow below 52 °C and dark yellow above 52 °C [11].

 $2AgI + HgI_2 \rightarrow Ag_2HgI_4$ 

2.2.2 Preparation of Doped Sample  $[0.7(Ag_2HgI_4):0.3(AgI_x:CuI_{(1-x)})]$ 

AgI and CuI were mixing in various x=0.2, 0.4, 0.6 and 0.8 mol. wt. % respectively in an Agate motar to form (AgI $_x$ :CuI $_{(1-x)}$ ) composite mixture by solid state reaction. Now Silver tetraiomercurate 0.7 mol. wt. % [Ag $_x$ +HgI $_4$ ]

\*Corresponding Author
Email Address: sabaamu@gmail.com (Noorus Saba)

were doped by 0.3 mol. wt. % (AgI<sub>x</sub>:CuI<sub>(1-x)</sub>) composite mixture to form  $[0.7(Ag_2HgI_4):0.3(AgI_x:CuI_{(1-x)})]$  fast ion conductor, in an Agate mortar at room temperature and heating them at 200 °C (473K) for 24 h in a silica crucible. After intermittent grinding, all the samples were prepared [12].

#### 2.3. Characterization of Pure and Doped Samples

#### 2.3.1 X-Ray Powder Diffraction Studies

X-ray powder diffraction were performed for all the fast ionic composite systems  $[0.7(Ag_2HgI_4):0.3(AgI_x:CuI_{(1-x)})]$  x = 0.2, 0.4, 0.6 and 0.8 mol. wt.% respectively after the reaction was completed using Rigaku Rad B powder diffractometer with a K-beta filter with Cu-K $\alpha$  ( $\lambda$ =1.54060 Å) radiation at room temperature. The angle range for measurement was from 10 °C to 80 °C and the scanning speed was 1°min-1. The x-ray diffractogram values of all the composite [0.7(Ag2HgI4):0.3(AgIx:CuI(1-x))] correspond to standard values of [Ag<sub>2</sub>HgI<sub>4</sub>] and careful analysis revealed that in addition to standard peaks of pure host [Ag<sub>2</sub>HgI<sub>4</sub>], a number of peaks appeared for the (AgI<sub>x</sub>:CuI<sub>(1-x)</sub>)doped host composite system.

#### 2.3.2 FTIR Measurements

The IR spectrum was recorder for all the fast ionic composite systems [0.7(Ag<sub>2</sub>HgI<sub>4</sub>):0.3(AgI<sub>x</sub>:CuI<sub>(1-x)</sub>)] (where x = 0.2, 0.4, 0.6 and 0.8 mol. wt. % respectively) in the mid-infrared range 400-4000 cm<sup>-1</sup> (25-25  $\mu m$ ) at room temperature using a INTERSPEC-2020, FTIR spectrophotometer measured in KBr.

#### 2.3.3 Thermal Analysis

Differential thermal analysis (DTA) was carried out on  $[0.7(Ag_2HgI_4):0.3(AgI_x:CuI_{(1:x)})]$  mixed composite samples, using a universal Schimadzu SC - TA-60 thermal analyzer equipped with disk memory and data analyzer in the temperature range 20 °C - 500 °C, with the powder sample sealed in pt capsules at heating rates of 10 °C min-1/air medium. Temperature calibration was prepared using a standard 'In' sample. Before carryings out the DTA, the samples was dried in a vacuumed oven for an hour at 100 °C and then cooled down to room temperature, thereafter sample was equilibrated at 20 °C for 10 min.

Differential scanning calorimetry (DSC) and thermo-gravimetric analysis (TGA) was carried out on  $[0.7(Ag_2HgI_4):0.3(AgI_s:CuI_{(1:x)})]$  mixed composite samples, using DTG-60H thermal analyser in nitrogen atmosphere with flow rate of 30 mLmin $^{-1}$  and heating rate 25 °C min $^{-1}$  in the temperature range 20 °C - 500 °C. The reference used was 10 mg alumina powder.

#### 3. Results and Discussion

## 3.1 FTIR Analysis

#### 3.1.1 FTIR Discussion in Ag<sub>2</sub>HgI<sub>4</sub>

As in Ketelaar description, the  $\alpha$ -phase retains the same iodine structure as in the  $\beta$  phase. While the cation and vacancy sites becomes equivalent [13]. Later studies showed that the low temperature phases are tetragonal and in addition, are not isostructural, differing in the placement of the two monovalent cation (Ag or Cu) and vacancy [14, 15]. Thus based on data from the best single crystals, i.e. tetragonal  $\beta$ - phase was the only stable low-temperature phase and the apparent phase change after cycling could be explained by the formation of domains with the tetragonal c axis randomly oriented along the three spatial axes, thus giving the impression of a cubic lattice. The interpretation of a single low-temperature phase has the broadest base of support of the two views at present [15]. Assuming the  $\beta$  phase is tetragonal, the number and symmetry of normal modes can be determined. Group theory analysis finds the following number and symmetries for the 18 optical modes in Ag<sub>2</sub>HgI<sub>4</sub> materials.

Ag<sub>2</sub>HgI<sub>4</sub>: 3A+ 5B+ 5E

The Infrared and Raman selection rules give the following allowed mode symmetries.

Infrared - Ag<sub>2</sub>HgI<sub>4</sub>: 5B+ 5E (10 Bands)
Raman - Ag<sub>2</sub>HgI<sub>4</sub>: 3A+ 5B+ 5E (13 Bands)

Using projection operators, we find that the B symmetry mode involve motion of the cation along the tetragonal c axis (z), and the E modes involve motion of the cations, along the a and b axes (x or y), B mode couple to electric fields along the z axis and E modes couple to fields in the xy plane, so that FTIR spectra would determine the mode-symmetry assignments uniquely [16-19].

#### 3.1.2 Factor Group Analysis of Ag<sub>2</sub>HgI<sub>4</sub>

The irreducible representation for the 15 IR allowed modes are listed in Table 1.

Table 1 The irreducible representation for the 15 predicted modes of 8- Ag<sub>2</sub>HgI<sub>4</sub>

	Ag <sub>2</sub> HgI <sub>4</sub>
Internal modes (HgI <sub>4</sub> )	
Stretch	A+B+E
Deformation	
External modes (HgI4)	
Rotatory	A+E
Translational	B+E
External Modes (Cu or Ag)	
Translational	B+E
Acoustic Modes	B+E

The unit cell group analysis of  $Ag_2HgI_4$  is also shown in Table 1 [18], with the  $D_{2d}$  -  $S_4$  correlation being  $A_1$  and  $A_2$  to A, B and  $B_2$  to B and E to E. Fig. 1 shows FTIR spectrum for  $[0.7(Ag_2HgI_4):0.3(AgI_x:CuI_{(1-x)})]$  fast ionic conductors where  $x=0.2,\,0.4,\,0.6$  and 0.8 mol. wt. %.

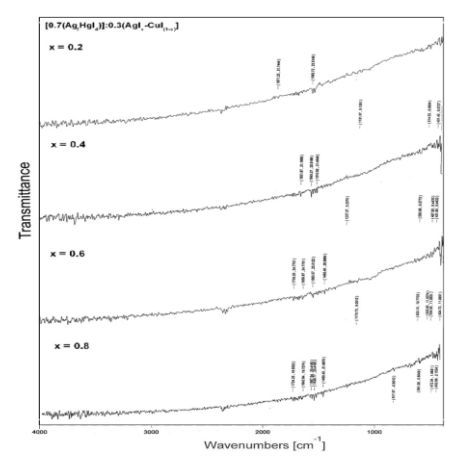


Fig. 1 FTIR spectrum for  $[0.7(Ag_2HgI_4):0.3(AgI_x:CuI_{(1-x)})]$  fast ionic conductors, where (x=0.2,0.4,0.6 and 0.8 mol. wt. %)

In the IR spectra of  $[0.7(Ag_2HgI_4):0.3(AgI_{0.8}:CuI_{0.2})]$  the 2351 cm<sup>-1</sup> peak in Table 1 is strongest in xx, yy and zz direction making it an A. The A peak shifted in x = 0.4, 0.6 and 0.8 at 2322, 2244, 2389 cm<sup>-1</sup>. The peak at 1460  $cm^{\mbox{\tiny -1}}$  and 1396  $cm^{\mbox{\tiny -1}}$  are strongest in the xx and yy polarizations and therefore belongs to A or B classes. This peak shifted in x = 0.4, 0.6 and 0.8 mol. wt. % composites are  $1385 \text{ cm}^{-1}$  for x = 0.4, 1385.01,  $1333.42 \text{ cm}^{-1}$  for x = 0.6 and 1508.02 cm<sup>-1</sup> for x = 0.8 mol. wt. %. The only noticeable peaks in xz polarization and E symmetry is at 424 cm<sup>-1</sup> and the 789 cm<sup>-1</sup> shoulder appears to be weak in xx, zz and xz polarization making it likely that at least some of the peaks causing this feature would be maximized in the xy polarization and therefore of B symmetry in x = 0.2 mol. wt. %. E symmetry peaks are found in x = 0.4, 0.6 and 0.8 are at 416 cm<sup>-1</sup>, 420.76 cm<sup>-1</sup> and 440.60 cm<sup>-1</sup>. The shoulder peaks appears in x = 0.4, 0.6 and 0.8 are 1083.43, 1000 and 1111.21 cm<sup>-1</sup> respectively. The E peaks leaves some weak peaks at 464.40, 515.99 and 639.00 cm<sup>-1</sup> in x = 0.2 which shifted in x= 0.4, 0.6 and 0.8 are at (460.44 cm<sup>-1</sup>), (496.15 and 662.81 cm<sup>-1</sup>) and (500.12, 539.80 cm<sup>-1</sup>) respectively.

**Table 2**  $[0.7(Ag_2HgI_4):0.3(AgI_x:CuI_{(1-x)})]$  (where x = 0.2, 0.4, 0.6 and 0.8 mol. wt. %.) room temperature peaks and assignments.

[0.7(Ag <sub>2</sub> HgI <sub>4</sub> ):0.3 [0.7(Ag <sub>2</sub> HgI <sub>4</sub> ):0.3		[0.7(Ag <sub>2</sub> HgI <sub>4</sub> ):0.3(Ag		[0.7(Ag <sub>2</sub> HgI <sub>4</sub> ):0.3(A			
$(AgI)_{(0.8)}$	$:CuI_{(0.2)})]$	$(AgI)_{(0.6)}$ :	$_{6)}$ :CuI <sub>(0.4)</sub> )] I) <sub>(0.4)</sub> :CuI <sub>(0.6)</sub> )]		$gI)_{(0.2)}:CuI_{(0.8)})]$		
Peaks	Assign	Peaks	Assign	Peaks	Assignm	Peaks	Assignm
(cm <sup>-1</sup> )	ments	(cm <sup>-1</sup> )	ments	(cm <sup>-1</sup> )	ents	(cm <sup>-1</sup> )	ents
2381	A	2352	A	2299	A	2321	A
1539	A	1563.57	A	1563.27	A	1562	A
817	?	-	?	1551	?	1052	?
1460	В	1170.73	В	1510.92	В	-	В
432	В	1460.40	В	431	В	431.45	В
		424.72					

Unassigned and a speculatively assignment for the 789 cm $^{-1}$  feature. HgI $_2$  contamination peaks also found in at 623.13, 960, 662.81 and 539.80 cm $^{-1}$  for x = 0.2, 0.4, 0.6 and 0.8 respectively. Peaks of B and E symmetry are allowed in the IR spectra and should be strong peaks. The occurrence of 422.66 cm $^{-1}$  for [0.7(Ag $_2$ HgI $_4$ ):0.3(AgI $_3$ :CuI $_{(1-x)}$ )] in the IR strengthens the

E assignment for the peak at 424.72 cm $^{-1}$ . For the x = 0.4, 0.6 and 0.8, the peaks are at 406.79, 419.79, 439 cm $^{-1}$  in  $[0.7(Ag_2HgI_4):0.3(AgI_x:CuI_{(1-x)})]$  respectively (Table 2).

#### 3.1.3 FTIR Comparison in Ag<sub>2</sub>HgI<sub>4</sub>

From Table 3, the vibrational modes can be assigned by considering  $Ag_2HgI_4$  as consisting of the vibrational modes of AgI and  $(HgI_4)^{2-}$  species. In fact, as shown in Fig. 1, almost all the bands due to AgI and  $(HgI_4)^{2-}$  are seen in the pure  $Ag_2HgI_4$  composites. The band at  $1601~\text{cm}^{-1}$  can be assigned to the symmetric stretching "A" mode of  $(HgI_4)^{2-}$  species and this band is the strongest band at room temperature [20]. This assignment is in good agreement with the other  $(HgI_4)^{2-}$  tetrahedral compounds [1]. On the doping of  $(Ag^*_{-0.8}:Cu^*_{-0.2})$  ions in the pure  $Ag_2HgI_4$ , all six bands shifted to 424, 464, 515, 639, 1556 and  $1611~\text{cm}^{-1}$ . The  $1000-1500~\text{cm}^{-1}$  region consists of two bands at the positions  $1396~\text{cm}^{-1}$  and  $1460~\text{cm}^{-1}$  at room temperature and at low temperature, these bands are expected to split.

It is known from the IR spectra of (Ag+0.8:Cu+0.2)-ions conductors that this region consists of mostly of Ag-I [2] stretching modes. Hence, in all [0.7(Ag<sub>2</sub>HgI<sub>4</sub>):0.3(AgI<sub>x</sub>:CuI<sub>(1-x)</sub>)] composite samples, also the bands in this region can be assigned to symmetric stretching modes of Ag-I. Below 700 cm<sup>-1</sup>, there are five sharp bands at 427, 449, 470, 493 and 520 cm<sup>-1</sup> in pure Ag<sub>2</sub>HgI<sub>4</sub> [20], while species vibrations, the bands at 424, 464, 515, 639 cm  $^{1}$ , 416 and 460 cm $^{-1}$ , 420, 496 and 662 cm $^{-1}$  and 440, 500, 539, 477 cm $^{-1}$  in x = 0.2, 0.4, 0.6 and 0.8 (Ag<sup>+</sup>:Cu<sup>+</sup>)-ions conductors respectively, it is known from factor group analysis studies [16] that the bands in this region are due to deformation type metal-iodine vibrations. On comparison with (HgI<sub>4</sub>)<sup>2-</sup> species vibrations, the bands at 520 and 493 cm<sup>-1</sup> in pure Ag<sub>2</sub>HgI<sub>4</sub>, and 639 cm<sup>-1</sup> and 515 cm<sup>-1</sup>, 662 cm<sup>-1</sup> and 539 cm<sup>-1</sup> and 612 and 532 cm<sup>-1</sup> in x = 0.2, 0.6 and 0.8 (Ag<sup>+</sup>:Cu<sup>+</sup>)-ions conductors respectively (These bands are absent in x = 0.4 (Ag $^+$ :Cu $^+$ )-ions conductor) can be assigned to Cd-I deformation type bands. The band at 470 cm<sup>-1</sup> in pure Ag<sub>2</sub>HgI<sub>4</sub>, and 464, 460, 496 and 500 cm<sup>-1</sup> in x = 0.2, 0.4, 0.6 and 0.8 mol. wt. % (Ag<sup>+</sup>:Cu<sup>+</sup>)doped ions conductors respectively, is attributed to the E symmetry of Ag+ translational mode and is the characteristic attempt frequency of Ag+ ion arising from the diffusive behaviour to oscillatory behaviour. This assignment is well explained by Shriver [19] by referring to the negative pressure dependence and also using theoretical calculations. The value assigned to the attempt frequencies in  $Ag_2HgI_4$  is similar to cation transition modes in other related (Ag+:Cu+)-doped fast ionic conductors [19,20]. Another possibility is that motion of very large amplitude (diffusive like) is able to create configurational disorder which allows all IR modes [3].

 $\label{eq:table 3 [0.7(Ag_2HgI_4):0.3(AgI_x:CuI_{(1:x)})] fast ion conductors, where (x = 0.2, 0.4, 0.6 and 0.8 mol. wt. \%), room temperature peaks and assignment$ 

Far-IR tran	Assignment				
[0.7(Ag <sub>2</sub> H	[0.7(Ag <sub>2</sub> H	[0.7(Ag <sub>2</sub> HgI	[0.7(Ag <sub>2</sub> H	Symmetry	<del></del>
gI <sub>4</sub> ):0.3(A	gI <sub>4</sub> ):0.3(A	4):0.3(AgI) <sub>(0.</sub>	gI <sub>4</sub> ):0.3(A		
gI) <sub>(0.8)</sub> :CuI	gI) <sub>(0.6)</sub> :CuI	4):CuI(0.6))]	gI) <sub>(0.2)</sub> :CuI		
(0.2))]	(0.4))]		(0.8)		
2381	2352	2299	2321	A	HgI <sub>4</sub> <sup>2-</sup> Symmetric
					stretch
1539.77	1563.57	1563.27	1562.72	A	HgI <sub>4</sub> <sup>2</sup> ·
					deformation, Cu-
					I, Ag-I stretching
817	1170.73	1551	1052	В	deformation
1460.60	1460.40	1510.92	431.45	Е	M-I symmetric
					stretch
432.68	424.72	431.65		Е	M+ attempt
					frequency

Inspection of Table 3 and Fig. 1, shows that IR spectra of all  $[0.7(Ag_2HgI_4):0.3(AgI_x:CuI_{(1:x)})]$  and conductors exhibit the strongest feature at ca 1611.19, 1607.22, 1603.26 and 1611.19 cm $^{-1}$  respectively, while the infrared activity below 900 cm $^{-1}$  is weak. On the basis of the above discussion, these results strongly suggest that the existence of  $(HgI_4)_2^2/(Ag^*:Cu^*)$  tetrahedral in the x = 0.2 and 0.8 mol. wt. % (Ag\*:Cu\*)-doped fast ionic conductors should be excluded at least in concentration detectable by infrared spectroscopy.

Therefore, it is found that the infrared activity of the x = 0.2 and x = 0.8 mol. wt. % (Ag+:Cu+)-fast ionic conductors arises from  $(HgI_4)^2$  tetrahedral, while x = 0.4 mol. wt. % (Ag+:Cu+)-fast ionic conductors show weakest feature at lower frequencies. Increasing the Ag+:Cu+ content induces a decreases to increase of the infrared activity in  $[0.7(Ag_2HgI_4):0.3(AgI_x:CuI_{(1-x)})]$  [20].

#### 3.2 X-Ray Diffraction

Fig. 2 shows the typical XRD diffractogram obtained for Ag<sub>2</sub>HgI<sub>4</sub> ternary halides doped with different compositions of [0.7(Ag<sub>2</sub>HgI<sub>4</sub>):0.3(AgI<sub>x</sub>:CuI<sub>(1-x)</sub>)] composites (where x = 0.2, 0.4, 0.6 and 0.8 mol. wt. %). In  $\gamma$ -AgI, iodide ions are known to form a mixture of close packed structures, at temperatures well below 420 K (140 °C) consisting of fcc and hcp structures which are commonly designated as  $\gamma$ -AgI and  $\beta$ -AgI respectively. However, for pedagogical reasons only  $\gamma$ -AgI is considered at room temperature. According, to the xrd data obtained during the present study have been compared with that of  $\gamma$ -AgI.

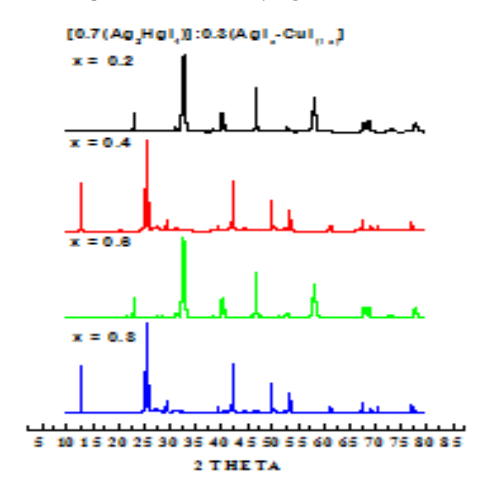


Fig. 2 X-ray diffractogram for  $[0.7(Ag_2HgI_4):0.3(AgI_x:CuI_{(1-x)})]$  fast ion conductors

**Table 4** X-ray diffractogram peaks and assignment for  $[0.7(Ag_2HgI_4):0.3(AgI_x:CuI_{(1-x)})]$  fast ion conductors

[0.7(Ag <sub>2</sub> HgdI <sub>4</sub> ):0.3(Ag I) <sub>(0.8)</sub> :CuI <sub>(0.2)</sub> )]		[0.7(Ag <sub>2</sub> HgI <sub>4</sub> ):0.3(AgI) <sub>(0.6)</sub> :CuI <sub>(0.4)</sub> )]		[0.7(Ag <sub>2</sub> HgI <sub>4</sub> ):0.3(A gI) <sub>(0.4)</sub> :CuI <sub>(0.6)</sub> )]		[0.7(Ag <sub>2</sub> HgI <sub>4</sub> ):0.3(A gI) <sub>(0.2)</sub> :CuI <sub>(0.8)</sub> )]	
2θ	Peak Assignment	2θ	Peak Assignment	2θ	Peak Assignment	2θ	Peak Assignment
22.22	AgI	22.94	γ-AgI	17.31	γ- CuI	26.20	γ- CuI
23.86	Ag <sub>2</sub> HgI <sub>4</sub>	31.09	metallic silver	25.42	γ- CuI	69.53	γ- CuI
27.39	$Ag_2HgI_4$	52.77	metallic silver	34.91	γ- CuI		
29.41	CuI			67.26	CuIAg <sub>2</sub> HgI <sub>4</sub>	77.3	CuIAg <sub>2</sub> HgI <sub>4</sub>
31.42	AgIAg <sub>2</sub> HgI <sub>4</sub>			72.01	CuIAg <sub>2</sub> HgI <sub>4</sub>		
37.98	$Ag_2HgI_4$						
43.78	CuIAg <sub>2</sub> HgI <sub>4</sub>						
49.45	CuI						
59.53	$Ag_2HgI_4$						
64.07	AgI						
68.78	$Ag_2HgI_4$						

It is clear from Table 4 that all the xrd data contain  $2\theta$  values different from that of the starting materials. Also it is obvious from Table 4, that the above compositions are polycrystalline in nature consisting of a multiphase mixture of AgI phases. These phases have been identifies as follows.

a.  $[0.7(Ag_2HgI_4):0.3(AgI_{0.8}:CuI_{0.2})]$ -Doped Composites (where x = 0.2, 0.4, 0.6 and 0.8 mol. wt. %)

In case of [0.7(Ag<sub>2</sub>HgI<sub>4</sub>):0.3(AgI<sub>0.8</sub>:CuI<sub>0.2</sub>)]-doped composites system, the peaks at 20.04° 25.45°, 32.62° and 47.80° can be attributed to the presence of  $\gamma$ -AgI, whereas peaks observed at 24.34° and 40.60° have been compared with that of CuIAg<sub>2</sub>CdI<sub>4</sub>. In addition,  $\gamma$ -CuI lines have also been observed at 15.74° and 28.33°. Effectively the composition of [0.7(Ag<sub>2</sub>HgI<sub>4</sub>):0.3(AgI<sub>0.8</sub>:CuI<sub>0.2</sub>)]-doped composites system consists of  $\gamma$ -AgI, CuIAg<sub>2</sub>HgI<sub>4</sub>,  $\gamma$ -CuI, AgIAg<sub>2</sub>HgI<sub>4</sub>, and pure Ag<sub>2</sub>HgI<sub>4</sub> phases [7].

b.  $[0.7(Ag_2HgI_4):0.3(AgI_{0.6}:CuI_{0.4})]$ -doped composites (where  $x=0.2,\,0.4,\,0.6$  and 0.8 mol. wt. %)

In case of [0.7(Ag<sub>2</sub>HgI<sub>4</sub>):0.3(AgI<sub>0.6</sub>:CuI<sub>0.4</sub>)]-doped composites system, the peaks observed at 19.02°, 31.21°, 22.94° and 23.22° alone could be attributed to the presence of  $\gamma$ -AgI in [0.7(Ag<sub>2</sub>HgI<sub>4</sub>):0.3(AgI<sub>0.6</sub>:CuI<sub>0.4</sub>)]. Another interesting feature of this particular compositions is that the xrd pattern is quite broad in shape thus suggesting its highly disordered nature. However, small traces of silver aggregates may be present in this composite material. Since very faint lines observed at 30.52° and 62.21° could only be attributed to the presence of small traces of metallic silver in Ag<sub>2</sub>HgI<sub>4</sub> (Table 4) [7].

c.  $[0.7(Ag_2Hg_14):0.3(Ag_10_4:Cul_{0.6})]$ -doped composites (where x = 0.2, 0.4, 0.6 and 0.8 mol. wt. %)

The xrd data corresponding to the composition having (AgI $_{0.4}$ :CuI $_{0.6}$ )]-doped composites of Ag $_2$ HgI $_4$  system appears to suggest that  $\gamma$ -CuI may be the major content in the dopant materials because of the fact that lines observed at  $2\theta = 43.53^{\circ}$ ,  $49.95^{\circ}$  and  $58.24^{\circ}$  could be fittingly attributed to the presence of  $\gamma$ -CuI. However, peaks observed at  $2\theta = 64.19^{\circ}$  and  $73.35^{\circ}$  can be attributed to the presence of CuIAg $_2$ HgI $_4$  as a constituent in the multiphase system (Table 4) [7].

d.  $[0.7(Ag_2HgI_4):0.3(AgI_{0.2}:CuI_{0.8})]$ -doped composites (where x = 0.2, 0.4, 0.6 and 0.8 mol. wt. %)

In case of the sample having  $[0.7(Ag_2HgI_4):0.3(AgI_{0.2}:CuI_{0.8})]$ -doped composites system, the observed xrd peaks at  $22.61^{\circ}$  and  $44.66^{\circ}$  may be attributed to the formation of CuI while the peak at  $76.80^{\circ}$  could be attributed to the presence of CuIAg<sub>2</sub>HgI<sub>4</sub>. Remaining unidentified peaks may be due to the presence of certain silver based compounds. From the above xrd analysis it is clear that all composite fast ionic conductors have been formed during the present investigation (Table 4) [7].

#### 3.3 Thermal Analysis

#### 3.3.1 Differential Scanning Calorimetry (DSC)

Fig. 3 depicts the DSC thermograms recorded for the sixteen different samples in the mixed fast ionic composite systems [0.7(Ag\_2Hgl\_4):0.3(Agl\_x:Cul\_{(1-x)})] (where x = 0.2, 0.4, 0.6 and 0.8 mol. wt. %).

It is clear from Fig. 4 and Table 5, that endothermic peaks are observed for  $[0.7(Ag_2HgI_4):0.3(AgI_{0.2}:CuI_{0.8})]$  composite, exhibits three endothermic peaks at 365.87 K, 493.69 K and 527.87 K, that can be assigned to the partial decomposition of  $\epsilon\text{-}Ag_2HgI_4$  in AgI,  $HgI_2$  and  $\beta\text{-}Ag_2HgI_4$  [8],  $\gamma\text{-}\alpha$  phase transition of CuI (at 493.69 K), tends to notify the presence of AgI [24]. On the other hand the endothermic peak that appears at 527.87 K in the case of x = 0.2 mol. wt. % composition is found to compare well with the observed melting temperature of CuIAg\_2HgI\_4 composite [25]. The  $\beta\text{-}Ag_2\text{HgI}_4$  peaks also occurs at 368.73 K, 372.75 K and 378.37 K in x = 0.4, 0.6 and 0.8 mol. wt. % respectively. This transition increases on further doping. The  $\gamma\text{-}\alpha$ -CuI transition occurs at 493.31K in x = 0.4, where  $\gamma\text{-}\alpha$ -phase transition of AgI occurs at (478.04 K, 461.145 K) in DSC plot of x = 0.6, 0.8 mol. wt. %.

The endothermic peaks occurs at 516.6 K in the case of x=0.4 for CuIAg<sub>2</sub>HgI<sub>4</sub> composites, whereas in x=0.6, 0.8 mol. wt. %., the endothermic peaks appeared at 586.82 K, 494.84 K is found to compare well with the observed melting temperature of AgI - Ag<sub>2</sub>HgI<sub>4</sub> composites. A careful analysis of the xrd patterns in Fig. 2 also reveals the formation of various other phases apart from Ag<sub>2</sub>HgI<sub>4</sub>, AgI or CuI. Therefore, the DSC results have indicated the presence of major content phases in  $[0.7(Ag_2HgI_4):0.3(AgI_x:CuI_{(1-x)})]$  composite.

On the other hand the exothermic peaks obtained in dsc curves of all the composites are at 423 K, 453 K, 463.31 K and 463 K respectively. Clearly, the above mentioned exothermic peaks are comparable to that of  $\beta\text{-}\alpha$  phase transition of pure AgI ( $\approx 420$  K). The DSC results therefore suggest that the combination of the two starting materials namely (AgI:CuI) and Ag2HgI4 is complete for a composition around 50 mol. % Ag2HgI4 resulting in the formation of new substances which are probably Ag\* ion conductors having very small traces of AgI [21].

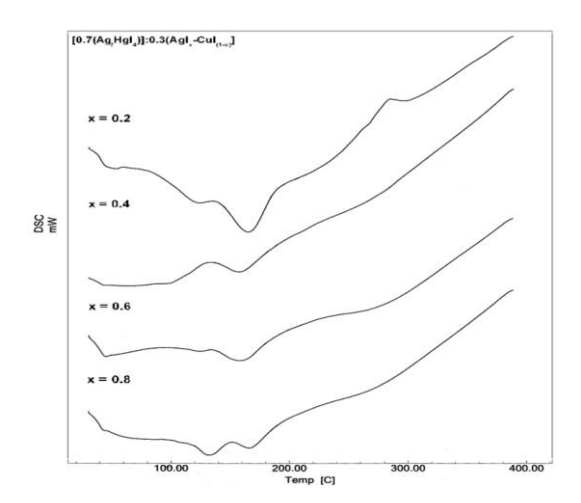


Fig. 3 DSC for  $[0.7(Ag_2HgL_4):0.3(AgJ_x:CuI_{(1-x)})]$  fast ionic conductors, (where x = 0.2,0.4, 0.6 and 0.8 mol. wt. %)

**Table 5** DSC endothermic peaks for  $[0.7(Ag_2HgI_4):0.3(AgI_x:CuI_{(1:x)})]$  fast ionic conductors (where x = 0.2,0.4, 0.6 and 0.8 mol. wt. %)

Composition	Endothermic Peaks (K)			
	I	II	III	
$[0.7(Ag_2HgI_4):0.3(AgI)_{(0.2)}:CuI_{(0.8)})]$	393	439.94	563	
$0.7(Ag_2HgI_4):0.3(AgI)_{(0.4)}:CuI_{(0.6)}]$	373	433.85	573	
$[0.7(Ag_2HgI_4):0.3(AgI)_{(0.6)}:CuI_{(0.4)})]$	393	434.87	553	
$[0.7(Ag_2HgI_4):0.3(AgI)_{(0.8)}:CuI_{(0.2)})]$	407	448.34	553	

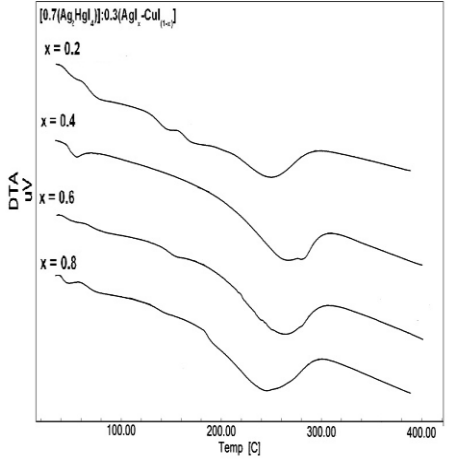


Fig. 4 DTA for  $[0.7(Ag_2HgI_4):0.3(AgI_x:CuI_{(1:x)})]$  fast ionic conductors (where x = 0.2, 0.4, 0.6 and 0.8 mol. wt. %)

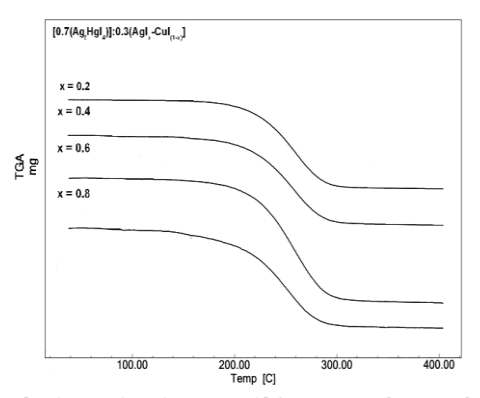


Fig. 5 TGA for  $[0.7(Ag_2Hgl_4):0.3(AgI_x:Cul_{(1-x)})]$  fast ionic conductors, where (x = 0.2, 0.4, 0.6 and 0.8 mol. wt. %).

#### 3.3.2 Differential Thermal Analysis (DTA)

DTA curves for all the sixteen samples composition  $[0.7(Ag_2HgL_4):0.3(AgL_x:Cul_{(1-x)})]$ , are shown in Fig. 4. On comparing these curves, we note the following important features.

- 1. A well-defined intense peak prepared at  $\sim\!353\text{-}393$  K in all curves. This peak corresponds to a  $\beta\text{-}\alpha\text{-}$  like transition of the host [Ag2HgI4]. The peak strength has increased on further doping of x mol. wt. % of (AgI:CuI). This is indicative of partial and complete stabilization of the high conducting  $\alpha\text{-}$  like phase of the host [22] in the samples respectively. These observations are exactly correlate our DSC results.
- 2. A second intense and well defined peak appeared at ~453-493 K in all the DTA curves of [0.7(Ag<sub>2</sub>HgI<sub>4</sub>):0.3(AgI<sub>x</sub>:CuI<sub>(1-x)</sub>)] system. This peak obviously corresponds to the  $\beta-\alpha$  like transition of CuI-AgI solid solutions, while in the DTA curves of Ag<sub>2</sub>HgI<sub>4</sub> this peak occurs at around ~513-553 K. This  $\beta-\alpha$  phase transition peak becomes broad with (AgI<sub>x</sub>:CuI<sub>(1-x)</sub>) content, this is due to the form of crystalline phase within space charge layer that is expected to form between (AgI:CuI) and [Ag<sub>2</sub>HgI<sub>4</sub>] (where x = 0.2, 0.4, 0.6 and 0.8 mol. wt. %) [23].
- 3. It has been observed from the DTA curves of  $[0.7(Ag_2HgI_4):0.3(AgI_x:CuI_{(1-x)})]$ , that an additional peak is obtained after the  $\beta$   $\alpha$  phase transition peak with the addition of  $(AgI_x:CuI_{(1-x)})$  and its intensity increase with the mole fraction of (AgI:CuI). This peak attributed to interface interactions between  $(AgI_x:CuI_{(1-x)})$  and  $[Ag_2HgI_4]$  (where x=0.2,0.4,0.6 and 0.8 mol. wt. %). The above results clearly reveal the partial presence of fast ionic phase in all the samples.

#### 3.3.3 Thermo Gravimetric Analysis (TGA)

TGA curves for  $(AgI_x:CuI_{(1-x)})$ -doped host samples, it shifts to a lower temperature because of the interaction between dopant  $(AgI_x:CuI_{(1-x)})$  and host  $[Ag_2:HgI_4]$  (where  $x=0.2,\ 0.4,\ 0.6$  and 0.8 mol. wt. %). In the TGA curves of  $[0.7(Ag_2:HgI_4):0.3(AgI_x:CuI_{(1-x)})]$  (Fig. 5), from room temperature up to about 400 °C. One distinct peak of TGA are obtained for the  $[0.7(Ag_2:HgI_4):0.3(AgI_x:CuI_{(1-x)})]$ , in the temperature range 400 °C -500 °C with corresponding mass loss for pure samples, and for  $(AgI_x:CuI_{(1-x)})$ -doped host samples [12] are shown. These data corroborate the observations of TGA studies.

#### 4. Conclusion

Thus, novel composite fast ion conductors  $[0.7(Ag_2HgI_4):0.3(AgI_x:CuI_{(1-x)})]$ , composite fast ion conductors were prepared and investigated also by X-ray powder diffraction, FTIR spectral analysis, differential thermal analysis (DTA), differential scanning calorimetry (DSC) and thermogravimetric analysis (TGA) studies to confirmed the formation of all the fast ion conductors.

### Acknowledgements

The authors are gratefully acknowledged to UGC New Delhi for financial assistance as UGC-PDF Women Scientist Scheme. The authors also thankful to Prof. Reshef Tenne and Dr. Feldmann at the Wiezmann Institute of Science (Israel) for obtaining the x-ray measurements of our pure and doped samples. The authors also gratefully acknowledge the Chairman of the Department of Chemistry for providing the research facilities.

#### References

- [1] J.B. Goodenough, Ceramic solid electrolytes, Solid State Ionics 94 (1997) 17-25.
- [2] S. Geller, Solid Electrolytes, Springer, Berlin, 1977.
- [3] S. Hull, Superionics: crystal structures and conduction processes, Rep. Prog. Phys. 67 (2004) 1233-1314.
- [4] R.C. Agrawal, R.K. Gupta, Transport property and battery discharge characteristic studies on 1-x(0.75Agl:0.25AgCl): xAl<sub>2</sub>O<sub>3</sub> composite electrolyte system, Jour. Mater. Sci. 30 (1995) 3612-3618.
- [5] R.B. Beeken, J.C. Faludi, W.M. Schreier, J.M. Tritz, Ionic conductivity in Cusubstituted Ag<sub>2</sub>CdI<sub>4</sub>, Solid State Ionics 154-155 (2002) 719-722.

- [6] Noorussaba, A. Ahmad, Composition-induced phase transition in a [Ag2Hg14:0.2AgI] mixed composite system doped with CuI, Cen. Europ. J. Chem. 8(6) (2010) 1227-1235.
- [7] R.C. Agrawal, R. Kumar, A fast Ag+ ion conducting mixed glass system: x[0.75AgI:0.25AgCI]:(1-x)[Ag20:CrO<sub>3</sub>], Transport property and battery discharge characteristic studies, J. Phys. D: Appl. Phys. 29 (1996) 156-162.
- [8] K. Funke, Agl-type solid electrolytes, Prog. Solid State Chem. 11 (1976) 345-402.
- [9] H.R.C. Jaw, M.A. Mooney, T. Novinson, W.C. Kaska, J.I. Zink, Optical properties of the thermochromic compounds disilver tetraiodomercurate(2-) and dicopper tetraiodomercurate(2-), Inorg. Chem. 26 (1987) 1387-1391.
- [10] T. Matsui, J.B. Wagner, High conductivity cuprous halide-metal halide systems, J. Electrochem. Soc. 124 (1977) 937 -940.
- [11] Noorussaba, A. Ahmad, Synthesis, characterization, fast ion transport and phase transition in a [Ag<sub>2</sub>Hgl<sub>4</sub>:0.AgI] type superionic mixed composite materials (x = 0.2, 0.4, 0.6 mol. wt. %), Anal. Bioanal. Electrochem. 3 (2011) 261-278.
- [12] Noorussaba, I.M. Khan, A. Ahmad, B. Özçelik, Preparation, ionic transport properties and characterization of [CdHgI<sub>4</sub>:0.2AgI]:0.xCuI fast ion conductor (x = 0.2, 0.4 and 0.6 mol. wt. %), Asian J. Res. Chem. 6 (2013) 996-1002.
- [13] H.W. Zandbergen, The crystal structure of  $\alpha$ -thallium hexaiodochromate,  $\alpha$  Tl4Crl<sub>6</sub>, Acta Cryst. B. 35 (1979) 2852-2855.
- [14] A.V. Franiv, O.S. Kushnir, I.S. Girnyk, V.A. Franiv, I. Kityk, M. Piasecki, K.J. Plucinski, Growth and optical anisotropy of Tl<sub>4</sub>Cdl<sub>6</sub> single crystals, Ukr. J. Opt. 14 (2013) 6-13.
- $[15] \quad D.S. \ Kalyagin, Y.E. \ Ermolenko, Y.G. \ Vlasov, Diffusion of Tl-204 isotope and ionic conductivity in Tl_4HgI_6 membrane material for chemical sensors, Rus. J. Appld. Chem. 81 (2008) 2172-2174.$
- [16] M. Hassan, M.S. Nawaz, Rafiuddin, Ionic conduction and effect of immobile cation substitution in binary system (AgI) 4/5-(PbI<sub>2</sub>) 1/5, Radiat. Eff. Defect. S. 163 (2008) 885-891.
- [17] K. Wakamura, Characteristic properties of dielectric and electronic structures in super ionic conductors, Solid State Ionics 149 (2002) 73–80.
- [18] R. Sudharsanan, T.K.K. Srinivasan, Radhakrishna, Raman and far IR studies on Ag<sub>2</sub>CdI<sub>4</sub> and Cu<sub>2</sub>CdI<sub>4</sub> superionic compounds, Solid State Ionics 13 (1984) 277-283.
- [19] A. Viswanathan, S. Austin Suthanthiraraj, Impedance and modulus spectroscopic studies on the fast ion conducting system CuI-Ag<sub>2</sub>MoO<sub>4</sub>, Solid State Ionics 62 (1993) 79-83.
- [20] E.A. Secco, A. Sharma, Structure stabilization: locking-in fast cation conductivity phase in TII, J. Phys. Chem. Sol. 2 (1995) 251-254.
- [21] K. Siraj, Rafiuddin, Study of ionic conduction and dielectric behavior of pure and K<sup>+</sup> doped Ag<sub>2</sub>CdI<sub>4</sub>, Soft Nanosci. Lett. 2 (2012) 13-16.
- [22] R.C. Agrawal, R. Kumar, A. Chandra, Transport studies on a new fast silver ion conducting system: 0.7[0.75AgI:0.25AgCI]:0.3 [yAg<sub>2</sub>O:(1- y)B<sub>2</sub>O<sub>3</sub>], Solid State Ionics 84 (1996) 51-60.
- [23] Noorussaba, Afaq Ahmad, phase transition in a [Ag2HgI4:0.2AgI] Mixed composite systems doped with KI, Rus. J. Electrochem. 49 (2013) 1065-1072.